American Mineralogist, Volume 68, pages 506–511, 1983

Isomolar and isostructural pseudo-liquidus phase diagrams for oceanic basalts

DON ELTHON

Department of Geosciences
University of Houston
Houston, Texas 77004

Abstract

Comparisons are made between isomolar and isostructural pseudo-liquidus phase diagrams. Trends of individual oxides within oceanic basaltic glasses are poorly defined in isostructural diagrams, but are much better defined in isomolar diagrams. These poorly-defined chemical trends in basaltic glasses in the isostructural diagrams are believed to be a consequence of variations in Na_2O contents of oceanic basalts and the manner in which Na_2O, or the albite component, is projected in these diagrams.

Introduction

Over the years, a dual experimental approach has been taken in the study of the origin of basaltic magmas. On one hand, the crystallization of simple, synthetic compositions has been extremely productive in demonstrating the basic tenets of basalt crystallization. An alternative approach, recognizing that basalts are chemically complex, has relied upon the melting relationships of natural basalts. This second approach is more geologically reasonable, but the chemical complexity of natural basalts presents certain difficulties in interpretation as well as experimental design. One method to help circumvent these interpretational problems is through the construction of pseudo-liquidus phase diagrams (Coombs, 1963; O'Hara, 1968a,b; Jamieson, 1970; Biggar *et al.*, 1971; Irvine, 1970; Walker *et al.*, 1972, 1979; Stolper, 1977, 1980; Presnall *et al.*, 1979; Elthon and Scarfe, 1983, and others). The underlying principle upon which these diagrams are based is that the minerals that crystallize from a magma are largely determined by the composition of the magma itself. Ideally, once a pseudo-liquidus phase diagram has been constructed, it is possible to geometrically display the chemical relationships among different basalts and to extend the phase relationships established in a limited number of basalts to other chemically related basalts.

The use of these pseudo-liquidus phase diagrams for evaluating the origin of oceanic basalts has developed to the stage where major differences of petrogenetic thought hinge upon relatively minor differences in the compositions of these basalts (compare Presnall *et al.*, 1979; Stolper, 1980; Elthon and Scarfe, 1983). When using these pseudo-liquidus phase diagrams, one must keep in mind their limitations. Some problems associated with the use of these pseudo-liquidus diagrams are discussed below along with a suggested modification to improve their application.

Construction of isostructural pseudo-liquidus phase diagrams

As a rule, the compositions of rocks and minerals are calculated into four minerals that form the apices of a tetrahedron. The olivine–clinopyroxene–plagioclase–silica tetrahedron is a suitable choice for oceanic basalts because it contains all of the major minerals relevant to oceanic basalt crystallization at low pressures except for the oxide minerals. The interpretation of chemical trends within this tetrahedron is simplified by projecting all compositions to or from one apex onto the opposing face of the tetrahedron or onto a plane that lies within the tetrahedron itself.

The pseudo-liquidus phase diagrams of Walker *et al.* (1979), which are commonly used in discussions of oceanic basalt petrogenesis, are used here to illustrate problems that are associated with the quantitative use of pseudo-liquidus phase diagrams as they are presently constructed. In the course of this study, not every system for constructing pseudo-liquidus diagrams has been investigated in the same detail as the Walker *et al.* diagrams, but reconnaissance examinations of these other systems indicate that the limitations found in the Walker *et al.* diagrams are present in the other systems as well.

The major element composition of a rock or mineral is computed into the four minerals that form the apices of the tetrahedron by a two-step process. The initial step consists of reducing the major element analysis to four components that are somewhat analogous to the CaO–MgO–Al_2O_3–SiO_2 system (see Table 1). The type of pseudo-liquidus phase diagrams developed by Walker *et al.* and others (see introduction) are *isostructural*, where the term *isostructural* refers to the characteristic that minerals projecting to the same point have the same general structure, *i.e.*, the olivines (forsterite–fayalite) project to the M_2S point, the orthopyroxenes (enstatite–ferrosilite) project to the MS point, the clinopyroxenes

0003–004X/83/0506–0506$02.00

Table 1.

FIRST STAGE:

Isostructural Diagrams: Walker et al. (1979)

A = Al_2O_3-like component = moles of (Al_2O_3 + Na_2O + K_2O)

C = CaO-like component = moles of (CaO + $2Na_2O$ + $2K_2O$)

M = MgO-like component = moles of (MgO + FeO + MnO + $2Fe_2O_3$)

S = SiO_2-like component = moles of (SiO_2-$2Na_2O$ - $2K_2O$)

Isomolar diagrams: this report

A = moles of (Al_2O_3 + Fe_2O_3)

C = moles of (CaO + Na_2O + K_2O)

M = moles of (MgO + FeO + MnO-TiO_2)

S = moles of (SiO_2)

SECOND STAGE:

Plagioclase* = A

Clinopyroxene = C-A

Olivine = (M-C+A)/2

Silica = $S - \frac{(M+A+3C)}{2}$

*In the isomolar diagrams, anorthite forms the fourth apical mineral

(diopside–hedenbergite) project to the CMS_2 point, and the feldspars (anorthite–albite) project to the CAS_2 point (see appendix of O'Hara, *et al.*, 1975).

Anorthite ($CaAl_2Si_2O_8$) and albite ($NaAlSi_3O_8$) have different molar proportions (CAS_2 *vs.* $\frac{C}{2}\frac{A}{2}$ S_3) of oxides even though they have the generalized plagioclase crystal structure. In order to get these two feldspar end-members to plot at the same point on isostructural diagrams, the following factors are introduced into the data reduction procedure. The number of moles of Na_2O + K_2O is multiplied by two and then added to the moles of CaO to form the C-component, the number of moles of Na_2O + K_2O is added to the amount of Al_2O_3 in forming the A-component, and two times the number of moles of Na_2O + K_2O is subtracted from moles of silica in forming the S-component (see Table 1). The purpose of these mathematical procedures is to make all of the feldspars plot at the same compositional point, which has the advantage of geometrical simplicity for determining critical planes, alkemade tetrahedra, and liquid lines of descent.

The second stage in projecting basaltic composition into these pseudo-liquidus diagrams is to recalculate these four components into the four end-member minerals that form the apices of the tetrahedron. This procedure is given at the bottom of Table 1.

The ideal objective in developing pseudo-liquidus phase diagrams would be to construct diagrams that can be used to quantitatively evaluate crystallization and melting processes and to interpret chemical trends among basalts. The compositions of basaltic glasses from the Indian, Atlantic, and Pacific Oceans (from Melson *et al.*, 1977), the project FAMOUS area (Bryan and Moore, 1977), the Mid-Cayman Rise (Thompson *et al.*, 1980; W. G. Melson, pers. comm., 1981) and a few "primitive" basalt compositions (Frey *et al.*, 1974; Bryan, 1979; Wood *et al.*, 1979) are used to evaluate chemical trends within the pseudo-liquidus phase diagrams. For these calculations it is assumed that $Fe^{3+}/Fe^{2+} = 0.10$.

The projection of these basaltic glasses onto the olivine–clinopyroxene–silica plane by the method of Walker *et al.* (1979) is shown in Figure 1. As noted by Walker *et al.*, these compositions approximately parallel the olivine + clinopyroxene + plagioclase + liquid pseudo-univariant curve. One might anticipate that within this group of basaltic glasses, those compositions projecting at the left-hand (silica-poor) end of the basalt cluster would be the least differentiated (with the highest MgO) and those glasses at the right-hand (silica-rich) end would be the most differentiated (with the lowest MgO) because the early crystallizing olivine + plagioclase + clinopyroxene would drive residual glass compositions towards silica enrichment as the glass becomes depleted in MgO. The percentage of normative silica in the Ol/Cpx/Sil plane versus MgO in the glass is shown in Figure 2. The data scatter across the diagram and do not show any well-defined trend towards enrichment in normative silica with decreasing MgO (correlation coefficient is equal to −0.169).

It would also be anticipated that TiO_2 (and other elements that are relatively incompatible in olivine, clinopyroxene, and plagioclase) would exhibit a progressive increase with increasing normative silica content. The TiO_2 *vs.* normative silica plot (Fig. 3), however, exhibits a broad scatter of data that does not indicate an increasing TiO_2 with increasing normative silica (correlation coefficient is equal to 0.003).

Sodium decreases with increasing normative silica in the isostructural diagrams (Fig. 4; r = −0.603). This trend is contrary to what might be anticipated to develop during the crystallization of oceanic basalts. Sodium is incompatible in both olivines and pyroxenes in oceanic basalts.

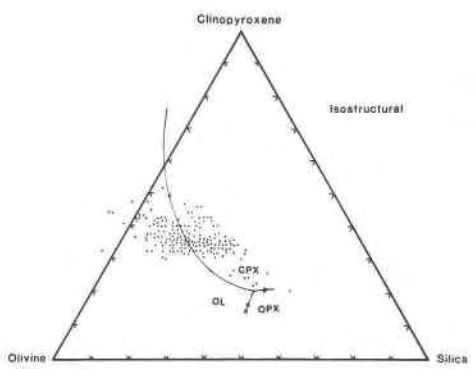

Fig. 1. Isostructural pseudo-liquidus phase diagram projected from plagioclase onto the olivine–clinopyroxene–silica plane. Isostructural projection method and 1 atm experimental data from Walker *et al.* (1979). Data points are oceanic basaltic glasses from the data sources given in the text.

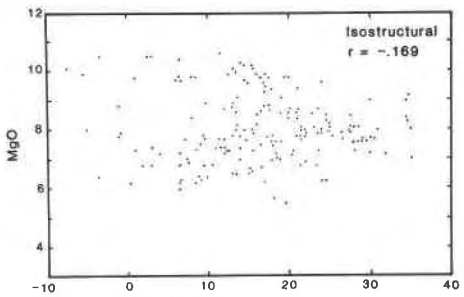

Fig. 2. Weight % MgO in basaltic glasses *vs.* the percentage of normative silica in the olivine–clinopyroxene–silica plane (Fig. 1). The percentage of normative silica = silica/(olivine+clinopyroxene+silica). Correlation coefficient = −0.169. Isostructural projection.

Additionally, the distribution coefficient for sodium between plagioclase and silicate liquids is less than one at temperatures greater than 1200°C and increases to 1.52 at 1100°C (Drake, 1976). The proportions in which these minerals crystallize in oceanic basalts is approximately 1 Ol:2 Plag along the Ol + Plag + Liq pseudo-divariant surface and approximately 1 Ol:9 Plag:9 Cpx along the Ol + Plag + Cpx + Liq pseudo-univariant curve, as deduced by least-squares regression of the experimental data of Walker *et al.* (1979) and Bender *et al.* (1978). Thus, even though sodium has a distribution coefficient greater than 1 at <1200°C for plagioclase, the sodium content of the liquid is still anticipated to gradually increase because the weighted distribution coefficient for olivine + plagioclase±clinopyroxene crystallization is still significantly less than 1.

Although it would be expected that MgO decreases and TiO_2 and Na_2O increase with increasing normative silica in oceanic basalt glasses, this expectation is not borne out by the data at hand, as projected onto isostructural diagrams.

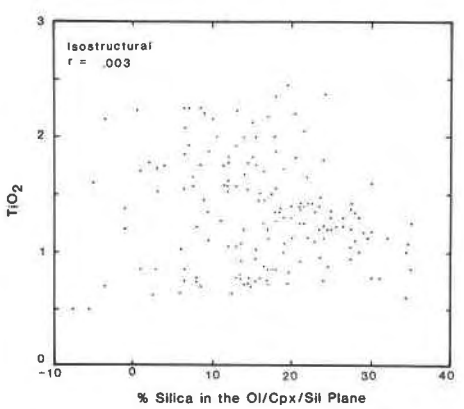

Fig. 3. Weight % TiO_2 in basaltic glasses *vs.* the percentage of normative silica in the olivine–clinopyroxene–silica plane (Fig. 1). Isostructural projection.

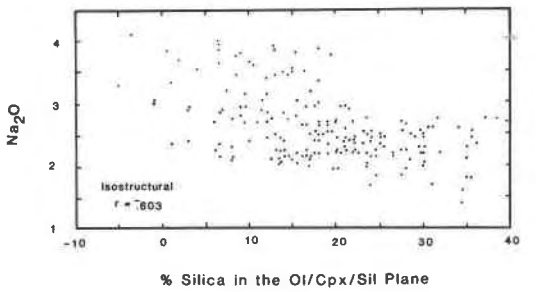

Fig. 4. Weight % Na_2O in basaltic glasses *vs.* the percentage of normative silica in the olivine-clinopyroxene-silica plane (Fig. 1). Isostructural projection.

This lack of definite chemical trends in basaltic glasses, when projected into isostructural pseudo-liquidus phase diagrams, becomes a handicap when evaluating the petrogenesis of oceanic basalts because these petrogenetic theories require the ability to distinguish where the least-differentiated basalts project within the basalt cluster (*e.g.*, Presnall *et al.*, 1979; Stolper, 1980; Elthon and Scarfe, 1983).

Construction of isomolar pseudo-liquidus phase diagrams

If pseudo-liquidus phase diagrams are going to be valuable for testing and refining petrologic theory, it is obvious that some improvements must be made in existing pseudo-liquidus diagrams. One change that significantly improves the chemical trends within the suite of oceanic basalts discussed above is to construct them on an *isomolar* basis rather than on an *isostructural* basis (see Table 1). In an isomolar projection, those minerals that have the same molar proportions of oxides project to one point. For olivines and pyroxenes, the projection is similar to the isostructural system in which olivines project to the M_2S point, orthopyroxenes to the MS point, and clinopyroxenes to the CMS_2 point. Plagioclase feldspars project along the $CAS_2 - \frac{C}{2}\frac{A}{2} S_3$ join rather than at a single point. Intermediate feldspars project along this join according to their An/(An+Ab+Or) ratio. In several respects, this projection procedure is similar to that used by Walker *et al.* (1972) for lunar rocks. The comparison between the spatial relations of minerals in this isomolar system and the isostructural type is shown in Figure 5.

The projection of the same set of basaltic glass analyses onto the Ol/Cpx/Sil plane of the *isomolar* system is shown in Figure 6. In this diagram the basaltic glasses form an elongate cluster near the 1 atm olivine + plagioclase + clinopyroxene + liquid pseudo-univariant curve.

Unlike the isostructural diagrams, there is a well-defined decrease in MgO (Fig. 7) and increase in TiO_2 (Fig. 8) and Na_2O (Fig. 9) with increasing normative silica (correlation coefficients equal to −0.907, 0.851, and 0.690, respectively) in the isomolar pseudo-liquidus phase diagrams. Those glasses that lie at the SiO_2-poor end of

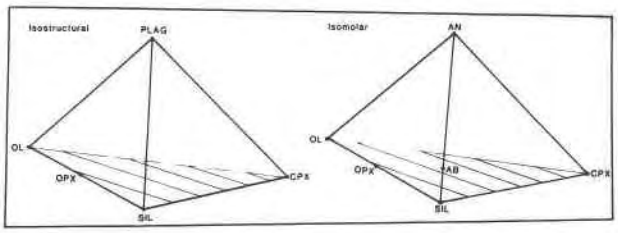

Fig. 5. Spatial relations of minerals in the isostructural (left) and isomolar (right) projections. See text for details.

the cluster have higher MgO and the lowest TiO_2, constituting the most "primitive" or least differentiated group of basalts. Those glasses that lie at the silica-rich end of the cluster have the lowest MgO and the highest TiO_2 and Na_2O contents and apparently have undergone the greatest degree of differentiation.

In these isomolar pseudo-liquidus phase diagrams, the spectrum of basalt compositions ranges from the least differentiated on the silica-poor end to the most differentiated on the silica-rich end. Thus, it appears that these isomolar diagrams more adequately display the compositional variations of oceanic basaltic glasses than their isostructural counterparts.

The use of these isomolar diagrams is, nonetheless, complicated by the fact that the plagioclase feldspars plot along the albite–anorthite join rather than at a single compositional point. Because the anorthite content of the feldspar changes during crystallization, more petrological information is needed to adequately trace plagioclase-controlled crystallization paths in isomolar diagrams than in isostructural diagrams. Consequently, in suites of oceanic basalts where no mineral chemistry or experimental results are available, tracing mineral-liquid crystallization paths with accuracy is extremely difficult. Where mineral chemistry or experimental results are available, it is possible to calculate these theoretical crystallization paths. Additionally, it is necessary to

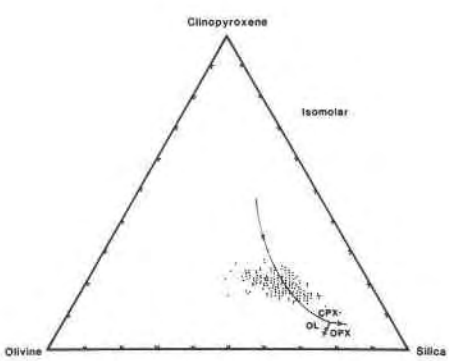

Fig. 6. Isomolar pseudo-liquidus phase diagram projected from anorthite onto the olivine–clinopyroxene–silica plane. 1 atm experimental data from Walker *et al.* (1979). Data points are oceanic basaltic glasses from sources listed in text.

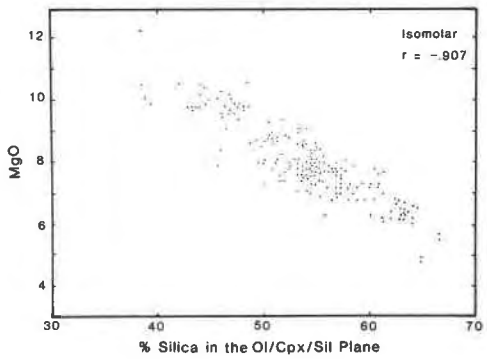

Fig. 7. Weight % MgO in basaltic glasses versus the percentage of normative silica in the olivine–clinopyroxene–silica plane (Fig. 6). The percentage of normative silica = silca/(olivine+clinopyroxene+silica).

know the plagioclase composition when defining certain geometrical features such as critical planes. If the composition of the feldspar is not known, these geometric features cannot be established with certainty. Consequently, the choice of using the isomolar rather than the isostructural diagrams to display either phase equilibria or basaltic compositions will depend upon the types of information that one wishes to extract from the diagrams.

Discussion

One reason for the much better defined chemical trend in the isomolar projections over the isostructural projections is related to the manner in which Na_2O and K_2O are projected in the isostructural system. The vectors in Figure 10 illustrate the effect of adding 1 mole% of each oxide to oceanic basalt glass VG-2 (Melson *et al.*, 1977). In the isomolar projections, each of the major element oxides has approximately the same magnitude of dislocation due to the addition of 1 mole% of each oxide,

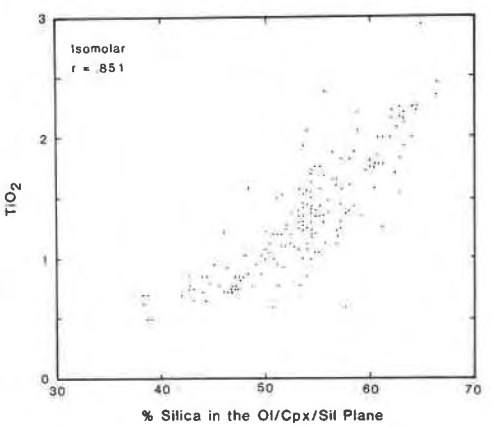

Fig. 8. Weight % TiO_2 in basaltic glasses *vs.* the percentage of normative silica in the olivine–clinopyroxene–silica plane (Fig. 6). Isomolar projection.

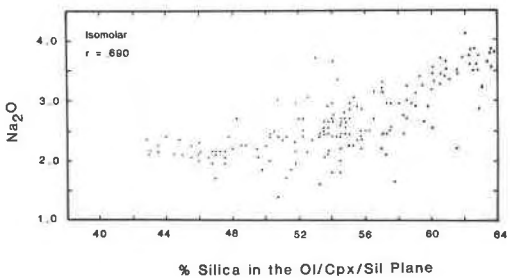

Fig. 9. Weight % Na_2O in basaltic glasses *vs.* the percentage of normative silica in the olivine–clinopyroxene–silica plane (Fig. 6). Isomolar projection.

although the direction may be different for individual oxides. In contrast, the amount of shift for $Na_2O + K_2O$ in the isostructural system is 4 to 8 times greater than that for the other oxides. One consequence of the exaggerated shifts for Na_2O and K_2O in these isostructural diagrams is that analytical uncertainties for these elements cause basaltic compositions to scatter in a trend that is subparallel to the 1 atm pseudo-univariant curve shown in Figure 1 (Presnall and Hoover, 1981; Bryan and Dick, 1982). The analytical uncertainties for these elements produce a much smaller scatter in the locations of basalt compositions in isomolar projections because of the smaller vectors for these oxides as shown in Figure 10.

As discussed above with reference to Figure 10, compositional variations in Na_2O or K_2O have a disproportionate effect on the locations of basalts on these phase diagrams. Figures 7, 8, and 9 show that, in isomolar projections, decreasing MgO and increasing TiO_2 and Na_2O are associated with increasing normative silica during differentiation in oceanic basaltic glasses, as expected from theoretical considerations. It appears that the poorly-defined chemical trends in isostructural projections (see Figs. 2, 3, and 4) are a consequence of the interplay between two opposing trends in isostructural diagrams. One trend, associated with decreasing MgO and increasing TiO_2 during differentiation, results in an increase in normative silica. The other trend, associated with increasing Na_2O during differentiation, results in a decrease in normative silica (see Fig. 10). The variations in Na_2O abundances in oceanic basalts, because of the strong effects that Na_2O has on the projected locations of basalts (Fig. 10), dominate over the other chemical variations associated with differentiation. The strong control that variations of Na_2O in basalts have on the projected locations of basalts in isostructural diagrams is indicated by the greater correlation between Na_2O and normative silica ($r = -0.603$) than between MgO or TiO_2 and normative silica ($r = -0.169$ and 0.003, respectively). Thus, the locations of individual basalts within isostructural pseudo-liquidus phase diagrams are very dependent on their Na_2O contents. It appears at this stage that the major reason for the lack of definite chemical trends in isostructural phase diagrams is that these two opposing trends compete against each other to produce a poorly-defined array of points on chemical variation diagrams.

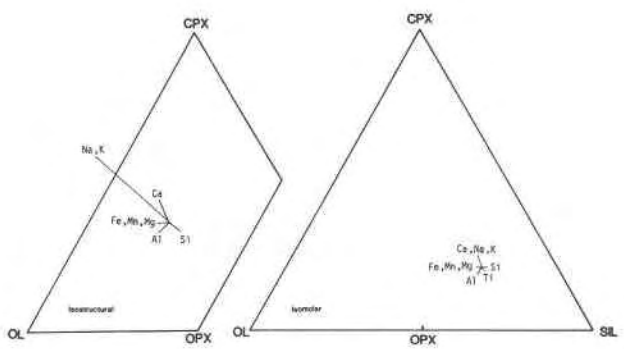

Fig. 10. Vectors showing the addition of 1 mole% of each of the major/minor element oxides to basaltic glass VG-2. Note the dramatic effect that Na_2O and K_2O have on the isostructural pseudo-liquidus diagrams.

Concluding remarks

Pseudo-liquidus phase diagrams have been and probably will continue to be a critical aspect in the interpretation of results from phase equilibria experiments on natural rocks. In the field of oceanic basalt petrology, petrogenetic theory has evolved to the state where minor differences in basalt compositions may imply major differences in their origin. Because of the subtleties involved in this problem, I suggest that the widely used isostructural phase diagrams need modification and improvement. By recalculating isostructural phase diagrams into their isomolar counterparts, a significant improvement in the chemical trends of oceanic basaltic glasses is observed. When using these isomolar diagrams, however, tracing plagioclase-controlled liquid lines of descent requires knowledge of the composition of the plagioclase that is crystallizing.

Although comparisons have been drawn between the isostructural pseudo-liquidus phase diagrams of Walker *et al.* (1979) and their isomolar counterparts, the report should not be misconstrued as a criticism of the methods or interpretation of Walker *et al.*; their conclusions regarding the effects of magma mixing would not be significantly modified by the substitution of isomolar for isostructural diagrams. Instead, this report represents an appeal to further refine pseudo-liquidus diagrams in order to more adequately display the chemical variations in basaltic magmas.

Acknowledgments

Comments by J. Butler, M. J. O'Hara, D. Presnall and D. Walker are appreciated. This work has been supported by the National Science Foundation through EAR 80-26445.

References

Bender, J. F., Hodges, F. N., Bence, A. E. (1978) Petrogenesis of basalts from the project FAMOUS area: Experimental study from 0 to 15 Kbars. Earth and Planetary Science Letters, 41, 277–302.

Biggar, G. M., O'Hara, M. J., Peckett, A., and Humphries, D. J. (1971) Lunar Lavas and the achondrites: petrogenesis of protohypersthene basalt in the mare lava lakes. Proceedings of the Second Lunar Science Conference, 617–664.

Bryan, W. B. (1979) Regional variation and petrogenesis of basalt glasses from the FAMOUS area, Mid-Atlantic Ridge. Journal of Petrology, 20, 293–325.

Bryan, W. B., Dick, H. J. B. (1982) Contrasted abyssal basalt liquidus trends: evidence for mantle major element heterogeneity. Earth and Planetary Science Letters, 58, 15–26.

Bryan, W. B. and Moore, J. G. (1977) Compositional variation of young basalts in the Mid-Atlantic Ridge rift valley near 36°49′N. Geological Society of America Bulletin, 88, 556–570.

Coombs, D. S. (1963) Trends and affinities of basaltic magmas and pyroxenes as illustrated on the diopside–olivine–silica diagram. Mineralogical Society of America, Special Paper 1, 227–250.

Drake, M. J. (1976) Plagioclase-melt equilibria. Geochimica et Cosmochimica Acta, 40, 457–465.

Elthon, D. and Scarfe, C. M. (1983) High-pressure phase equilibria of a high-magnesia basalt and the genesis of primary oceanic basalts. American Mineralogist, 68, in press.

Frey, F. A., Bryan, W. B. and Thompson, G. (1974) Atlantic Ocean seafloor: geochemistry and petrology of basalts from Legs 2 and 3 of the Deep Sea Drilling Program. Journal of Geophysical Research, 79, 5507–5527.

Irvine, T. N. (1970) Crystallization sequences in the Muskox intrusion and other layered intrusions, I. Olivine–pyroxene–plagioclase relations. Geological Society of South Africa Special Publication 1, 441–476.

Jamieson, B. G. (1970) Phase relations in some tholeiitic lavas illustrated by the system R_2O_3–XO–YO–ZO_2. Mineralogical Magazine, 37, 537–554.

Melson, W. G., Byerly, G. R., Nelen, J. A., O'Hearn, T., Wright, T. L. and Vallier, T. (1977) A catalog of the major element chemistry of abyssal volcanic glasses. Mineral Sciences Investigations: Smithsonian Contributions to the Earth Sciences, 19, 31–60.

O'Hara, M. J. (1968a) The bearing of phase equilibria studies on the origin and evolution of basic and ultrabasic rocks. Earth Science Reviews, 4, 69–133.

O'Hara, M. J. (1968b) Are ocean floor basalts primary magmas? Nature, 220, 683–686.

O'Hara, M. J., Saunders, M. J. and Mercy, E. L. P. (1975) Garnet peridotite, primary ultrabasic magma, and eclogite: interpretation of upper mantle processes in kimberlite. Physics and Chemistry of the Earth, 9, 571–604.

Presnall, D. C., Dixon, J. R., O'Donnell, T. H. and Dixon, S. A. (1979) Generation of mid-ocean ridge tholeiites. Journal of Petrology, 20, 3–35.

Presnall, D. C., Hoover, J. D. (1981) Analytical uncertainties and the problem of picritic versus tholeiitic primary magmas at mid-ocean ridges. Geological Society of America, Abstracts with Programs, 13, 533.

Stolper, E. (1977) Experimental petrology of eucritic meteorites. Geochimica et Cosmochimica Acta, 41, 587–611.

Stolper, E. (1980) A phase diagram for mid-ocean ridge basalts: Preliminary results and implications for petrogenesis. Contributions to Mineralogy and Petrology, 74, 13–23.

Thompson, G., Bryan, W. B. and Melson, W G. (1980) Geological and geophysical investigation of the Mid-Cayman Rise spreading center: geochemical variation and petrogenesis of basalt glasses. Journal of Geology, 88, 41–55.

Walker, D., Longhi, J. and Hays, J. F. (1972) Experimental petrology and origin of Fra Mauro rocks and soils. Proceedings of the Third Lunar Science Conference, 797–817.

Walker, D., Shibata, T. and DeLong, S. E. (1979) Abyssal tholeiites from the Oceanographer Fracture Zone. II. Phase equilibria and mixing. Contributions to Mineralogy and Petrology, 70, 111–126.

Wood, D. A., Tarney, J., Varet, J., Saunder, A. D., Bougault, H., Joron, J. L., Treuil, M. and Cann, J. R. (1979) Geochemistry of basalt drilled in the North Atlantic by IPOD leg 49: Implications for mantle heterogeneity. Earth and Planetary Science Letters, 42, 77–97.

Manuscript received, November 9, 1981;
accepted for publication, December 8, 1982.